DOI: 10.3969/j.issn.1673-3185.2017.06.006 **http:** // english.ship-research.com

Translated from: WU H L, ZHOU Q D, LV X J, et al. Flow noise prediction based on wavenumber-frequency spectrum of turbulent fluctuating pressure[J]. Chinese Journal of Ship Research, 2017, 12(6): 36-42.

Flow noise prediction based on wavenumber-frequency spectrum of turbulent fluctuating pressure

WU Hongliang[1], *ZHOU Qidou*[1], *LV Xiaojun*[1], *MENG Qingchang*[2]

1 Department of Naval Architecture Engineering, Naval University of Engineering, Wuhan 430033, China

2 College of Science, Naval University of Engineering, Wuhan 430033, China

Abstract: [Objectives] According to the Lighthill acoustic analogy equation and its development theory, it is feasible to analyze the wavenumber-frequency spectrum of turbulent wall pressure fluctuations, then make it an acoustic source in order to predict flow noise. Moreover, the study of the wavenumber-frequency spectrum is useful for understanding the temporal and spatial characteristics of turbulent structures. **[Methods]** Taking the NACA 0012 airfoil, which was studied by Brooks, as an example, we employ the Large Eddy Simulation (LES) method to calculate the flow field and obtain a numerical solution of the wavenumber-frequency spectrum via the Fourier transform. On this basis, we take the wavenumber-frequency spectrum as an input condition for predicting the radiated noise using the acoustic analogy equation of the Goldstein version. At the same time, acoustic software is used to calculate the flow noise. Comparing these two sets of results with Brooks' empirical formula, the sound pressure level is found to be within the same order of magnitude. **[Results]** The results show that the spectrum on an airfoil surface with a small curvature change is comparable with the Corcos spectrum model on a flat plate, and their general characteristics are similar. Finally, we conclude that the forecast results of the method in this paper accord better with Brooks' experimental results at low and medium frequencies. **[Conclusions]** This shows that it is necessary to carry out the study of wavenumber-frequency spectra, and it is reasonable to make it the main sound source in order to predict flow noise produced at subsonic speed.

Key words: wavenumber-frequency spectrum; Fourier transform; flow noise; acoustic analogy equation

CLC number: U661.44

0 Introduction

Turbulent fluctuating pressure is an important representation of the turbulent unsteady characteristic. It is also the main source of fluid induced structural vibration and noise generation. Corcos[1] first gave the wavenumber-frequency spectrum model of turbulent fluctuating pressure on a flat plate by Fourier transform to understand the temporal and spatial characteristics of turbulent structures and provide input conditions for the acoustic radiation prediction of flow noise. At present, the main methods for the research on turbulent fluctuating pressure and its wavenumber-frequency spectrum are experimental measurement and Fourier transform. The experimental research is time-consuming and laborious, and the object of experimental research is not universal.

Flow noise is the flowing Reynolds stress radiation noise, and can be divided into aerodynamic noise and hydrodynamic noise. It is mainly composed of two parts: the direct radiation noise of the turbulent boundary layer and the radiation noise generated by the structural vibration excited by the fluctuating pressure of the turbulent boundary layer. In this paper, we will mainly discuss the direct radiation noise in the turbulent boundary layer. In general, there are

Received: 2017 - 05 - 03

Supported by: National Natural Science Foundation of China (51309230); National Ministries Foundation

Author(s): WU Hongliang, male, born in 1992, master candidate. Research interest: hydrodynamic noise of ships. E-mail: 1404587678@qq.com

ZHOU Qidou (Corresponding author), male, born in 1962, professor, doctoral supervisor. Research interests: vibration and noise control, hydrodynamics. E-mail: qidou_zhou@126.com

two kinds of numerical prediction methods for direct radiation noise, i.e., direct method and indirect method. In the direct method, the unsteady flow and noise generated by it are calculated at the same time according to the control equation of the total flow field (Navier-Stokes (N-S) equation), including Direct Numerical Simulation (DNS), Large Eddy Simulation (LES), Reynolds-Averaged N-S (RANS), etc. The direct method is the most accurate method, will not be affected by the restriction of the conditions such as the flow state (e.g., low Mach number and high Reynolds number) or the sound source properties, and can calculate the generation and propagation of sound. However, the required solved area should be large enough, which at least fully includes the sound source area and its near-field area, which requires enormous computing resource. In the indirect method, the CFD method is first used to calculate the flow field, and then the far-field noise level is obtained by means of integration or acoustic analogy. The most basic assumption of the indirect method is to ignore the sound-flow coupling. In the method, the flow field and sound field are calculated, respectively. Therefore, it is more suitable for cases of low Mach number. Indirect methods mainly include turbulence model/acoustic analogy, discrete vortex method/acoustic analogy, RANS random noise generation model, viscous acoustic splitting method, linear Euler equation with source term, vortex sound theory, etc. In engineering, indirect method is generally adopted, i.e., the CFD program (FLUENT, STAR-CD, CFX, STAR-CCM+, Powerflow, etc.) is first used to obtain the flowing sound source, and then the flow noise is predicted by commercial flow noise simulation software. However, the computing code of commercial software is not open source, and the following problems have not been solved, such as, whether adaptive adjustment has been made for the aerodynamic characteristics in the flow noise calculation module based on the development of aeroacoustics, whether approximate treatment is conducted or whether empirical parameters have been introduced in the solving process [2]. Therefore, the development of hydrodynamic noise prediction technology has been severely constrained.

At present, for the acoustic radiation problem of the turbulent boundary layer, the related theories are based on the Lighthill acoustic analogy equation and the equations developed from it, e.g., the Curle equation considering solid boundary, Ffowcs Williams equation, Hawking equation, and the Goldstein acoustic analogy integral equation. However, there are different assumptions on the main sound source mechanism. The acknowledged assumptions include the dipole source of the wall fluctuating pressure, the quadrupole source of turbulent Reynolds stress, and the monopole source generated by the inhomogeneous mass/heat inflow in a fluid. Wang et al.[3] adopted the LES and acoustic infinite element method to numerically predict the submarine noise in the frequency domain, and believed that, compared with the plane sound source (dipole sound source), the contribution of the body sound source (quadrupole sound source) in the total sound level can be neglected. Pan et al.[4] studied the flow noise of the turbulent boundary layer of low Mach number, which has been fully developed on a rigid smooth flat plate, and separately discussed the contribution of the dipole and quadrupole sound sources to the flow noise. They found that, the fluctuation generated by the dipole was mainly concentrated in the low frequency band (<500 Hz), the fluctuation generated by the quadrupole was mainly concentrated in the middle and high frequency bands (1 200-2 500 Hz). They believed that the wall shear stress (dipole sound source) was the main source for the direct radiation noise in turbulent boundary layer. Ito[5] and Moritoh et al.[6] revealed through a large number of experiments that the fluctuating pressure generated during the train operation was the main source of aerodynamic noise. Xiao and Kang[7] predicted the aerodynamic noise of train head surface by using the LES combined with the Lighthill-Curle acoustic analogy theory. They also thought that the dipole source of low Mach number was the main source of aerodynamic noise. This was because the dipole source noise was proportional to the Mach number to the power of 3, while the quadrupole source noise was proportional to the Mach number to the power of 5. Therefore, at the subsonic speed, the quadrupole source noise could be negligible compared with the dipole source noise.

In this paper, we will take the three-dimensional airfoil as an example, only consider the dipole source radiation noise of the turbulent fluctuating pressure at the subsonic speed, and use the form of pressure spectrum as the sound source input. The main ideas are as follows: First, the flow field data are calculated by CFD simulation, and the numerical method of the wavenumber-frequency spectrum of the turbulent fluctuating pressure of arbitrary surface is established by Fourier transform. Then, the obtained wavenumber-frequency spectrum is substituted into the acoustic analog equation of the Goldstein version as the sound source to predict the radiation noise. Theoretically speaking, the method is also appropriate for the calculation of hydrodynamic noise.

1 Wavenumber-frequency spectrum model on a flat plate

For the fully developed turbulent layer on an infinite flat plate, it is assumed that the turbulent pressure field is uniform in space and is stationary relative to time. In other words, the spatial-temporal correlation of the wall pressure fluctuation only depends on the spatial distance and the time interval. Under the assumption, Corcos[1] proposed the wavenumber-frequency spectrum density model of wall pressure fluctuations as follows[8]:

$$S_{qq}(k,\omega_0)=S_0(\omega_0)\left(\frac{U_c}{\omega_0}\right)^2\hat{A}\left(1-\frac{k_s U_c}{\omega_0}\right)\hat{B}\left(\frac{k_t U_c}{\omega_0}\right) \tag{1}$$

where $S_0(\omega_0)$ is the point pressure frequency spectrum on the wall surface; ω_0 is the circular frequency of the pressure fluctuation, rad/s; $\hat{A}$ and $\hat{B}$ are the Fourier transforms of A and B (A and B are dimensionless functions obtained from the experiment); k_s and k_t are the wavenumbers of the flowing direction and the spanwise direction, respectively; and U_c is the convection velocity.

Brooks et al.[9] investigated the statistical properties of the hydrodynamic pressure field on a large enough flat plate, and provided the following experimental fitting functions of A and B:

$$A(\beta)=\mathrm{e}^{-\zeta_1|\beta|}$$
$$B(\beta)=\mathrm{e}^{-\zeta_2|\beta|} \tag{2}$$

where β is the independent variable of any function; ζ_1 and ζ_2 are adjustable coefficients, which can be obtained from the experiment, i.e.,

$$\zeta_1=0.11,\quad \zeta_2=0.6 \tag{3}$$

Substituting Eqs. (2) and (3) into Eq. (1), we can obtain the Corcos spectrum of the Brooks version, i.e.,

$$S_{qq}(k,\omega_0)=S_0(\omega_0)S_1(k_s)S_2(k_t) \tag{4}$$

where

$$S_1(k_s)=\frac{l_1}{\pi}\left[\frac{1}{1+l_1^2\left(\omega_0/U_c-k_s\right)^2}\right] \tag{5}$$

$$S_2(k_t)=\frac{l_2}{\pi}\left[\frac{1}{1+l_2^2k_t^2}\right] \tag{6}$$

The integral lengths of the flowing direction and the spanwise direction, l_1 and l_2, are defined by the following equations[9]:

$$\begin{cases} l_1=\dfrac{\int_0^\infty \xi_1 A\left(\omega_0\xi_1/U_c\right)\mathrm{d}\zeta_1}{\int_0^\infty A\left(\omega_0\xi_1/U_c\right)\mathrm{d}\zeta_1} \\ l_2=\dfrac{\int_0^\infty \xi_2 B\left(\omega_0\xi_2/U_c\right)\mathrm{d}\zeta_2}{\int_0^\infty B\left(\omega_0\xi_2/U_c\right)\mathrm{d}\zeta_2} \end{cases} \tag{7}$$

If we assume that the convection velocity U_c is constant, substituting Eqs. (2) and (3) into Eq. (7), we have

$$l_1=U_c/\zeta_1\omega_0,\quad l_2=U_c/\zeta_2\omega_0 \tag{8}$$

Based on the pressure spectrum $S_0(\omega_0)$ of a point on an infinite flat plate proposed by Chase[10], Howe [11] provided the following dimensionless form:

$$\bar{S}_0(\bar{\omega}_0)=\frac{6.140\,9\times10^{-6}\bar{\omega}_0^2}{\left(\bar{\omega}_0^2+0.014\,4\right)^{1.5}} \tag{9}$$

In the above equation, $\bar{S}_0(\bar{\omega}_0)=S_0(\omega_0)\cdot\left(U_0/\delta^*\right)/\left(0.5\rho_0U_0^2\right)^2$, where U_0 and ρ_0 are the uniform inflow velocity and the fluid density, respectively; $\bar{\omega}_0=\omega_0\delta^*/U_0$, where δ^* is the displacement thickness of the turbulent boundary layer. For fully developed turbulence on a flat plate, δ^* can be estimated by Eq. (10) [12]. In the equation, Re is the Reynolds number based on the arc length η_e starting from the leading edge.

$$\delta^*/\eta_e\approx0.047Re^{-1/5} \tag{10}$$

It is noted that the effects of the angle of attack α (unit: (°)) on the pressure surface and suction surface are

$$\begin{cases} \delta_p^*/\delta_0^*=10^{[-0.043\,2\alpha+0.001\,13\alpha^2]} \\ \dfrac{\delta_s^*}{\delta_0^*}=\begin{cases}10^{0.067\,9\alpha}, & 0^\circ\leqslant\alpha\leqslant7.5^\circ \\ 0.016\,2(10^{0.306\,6\alpha}), & 7.5^\circ\leqslant\alpha\leqslant12.5^\circ \\ 52.42(10^{0.025\,8\alpha}), & 12.5^\circ\leqslant\alpha\leqslant25^\circ\end{cases}\end{cases} \tag{11}$$

where the subscript "0" represents zero angle of attack, the subscript "p" represents the pressure surface of the boundary layer, and the subscript "s" represents the suction surface of the boundary layer.

Fig. 1 shows the wavenumber-frequency spectrum model of turbulent fluctuating pressure on an infinite plate proposed by Corcos[1]. In the figure, the vertical coordinate S_{qq} is the amplitude of the wavenumber-frequency spectrum, dB; k_sU_c/ω_0 and k_tc_0/ω_0 (c_0 is the sound speed) are the dimensionless wavenumbers of the flowing direction and spanwise direction, respectively. Since the general characteristics at different frequencies are consistent, while the amplitude values are different, the characteristic study of spectrum is mainly carried out here and we only provide the wavenumber-frequency spectrum at 1 200 Hz. From Fig. 1(b), we can see that, there is a peak in the spectrum when $k_s U_c/\omega_0 = 1$, which is consistent with the general characteristic that the wavenumber-frequency spectrum of the fluctuating pressure of the turbulent wall at a fixed frequency ($\omega_0 \delta^*/U >> 1$, where U is the inflow velocity) changes with the wavenumber in the flowing direction believed by Howe[11] (see Fig. 2). From the figure, we can see that there are two peaks when $k_s > 0$, the maximum peak appears in the "convection zone",

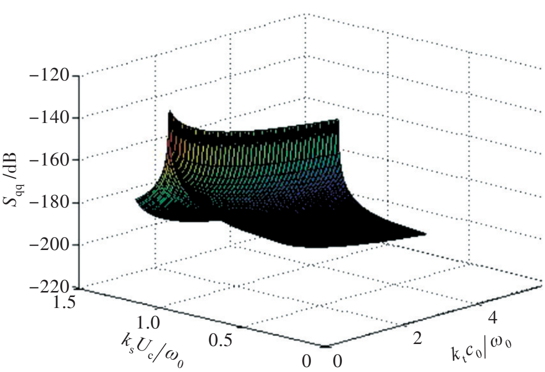

(a) Three-dimensional diagram of the wavenumber-frequency spectrum

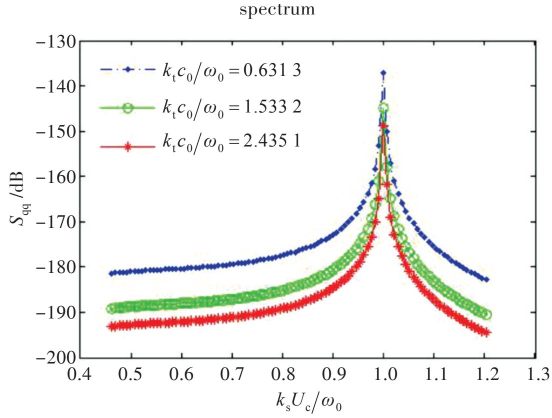

(b) Curve diagram of the wavenumber-frequency spectrum with the change of the wavenumber along the flowing direction

Fig.1 Wavenumber-frequency spectrum model on infinite plate of Corcos at frequency of 1 200 Hz

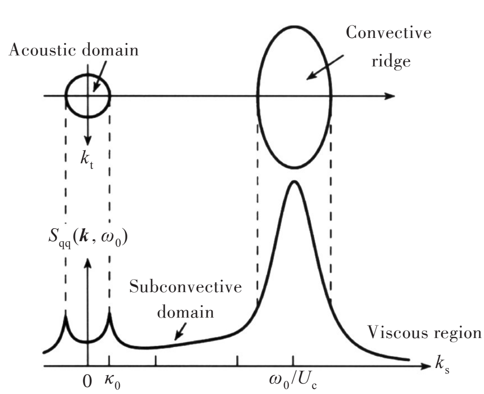

Fig.2 Characteristics of the wall fluctuating pressure spectrum

and most of the energy is transmitted by U_c. The turbulent energy in the region is said to exist in the convective ridge. The second peak appears near the acoustic wavenumber κ_0. With $\kappa_0 = \omega_0/c_0$ as the center, the range of $k < |\kappa_0|$ corresponds to the so-called "acoustic area" (where k is the modulus of the vector $\boldsymbol{k} = (k_s, k_t)$.

2 Acoustic prediction equation of the Goldstein version

When there is a solid boundary in the moving coordinate system, Goldstein[13] used the Green function method to study its sound production problems, and obtained the following basic governing equation:

$$p(\boldsymbol{x}, t) = \int_{-T}^{T} \iiint_{V(\tau)} \frac{\partial^2 G}{\partial y_i \partial y_j} \boldsymbol{T}'_{ij}(\boldsymbol{y}, \tau) \mathrm{d}\boldsymbol{y} \mathrm{d}\tau +$$

$$\int_{-T}^{T} \iint_{S(\tau)} \frac{\partial G}{\partial y_i} f_i \mathrm{d}S(\boldsymbol{y}) \mathrm{d}\tau + \int_{-T}^{T} \iint_{S(\tau)} \rho_0 V'_{\mathrm{n}} \frac{DG}{D\tau} \mathrm{d}S(\boldsymbol{y}) \mathrm{d}\tau \tag{12}$$

where $S(\tau)$ is the impenetrable solid surface; $V(\tau)$ is the exterior domain of $S(\tau)$; T is relatively large time; $\boldsymbol{T}'_{ij} = \rho v'_i v'_j + e_{ij}$, is the stress tensor of Lighthill in the isentropic flow, where e_{ij} is the (i, j) th component of the viscous stress tensor; $f_i = -n_i(p - p_0) + n_j e_{ij}$, is the i^{th} component of the force on unit area applied by the fluid boundary, where n_i is the i^{th} component of the unit inner normal $\boldsymbol{n}$ on surface of $S(\tau)$, p_0 is the pressure under the steady flow; and ρ_0 is the density under the steady flow. It is worth noting that there are two coordinate systems, i.e., the fixed coordinate system $\boldsymbol{y}'(y'_1, y'_2, y'_3)$ and the moving coordinate system $\boldsymbol{y}(y_1, y_2, y_3)$. v'_i and v'_j are the measured velocities in the fixed coordinate system, and $v'_i = v_i - \delta_{1i} U$, where v_i is the velocity in the moving coordinate system, δ_{ij} is the Kronecker delta function. The volume displacementterm $V'_{\mathrm{n}} = V_{\mathrm{n}} - n_1 U$, which is also a measured value in the fixed coordinate system, and satisfies the relationship $D/D\tau = \partial/\partial\tau + U(\partial/\partial y_1)$.

In the moving coordinate system, the solution of the Green function in Eq. (12) is

$$G(\boldsymbol{x}, t; \boldsymbol{y}, \tau) = \frac{1}{4\pi R} \delta[\tau + \frac{1}{\beta^2 c_0}(R + M(y_1 - x_1)) - t] \tag{13}$$

We take the Fourier transform of Eq. (13), and obtain the Green function in the frequency domain as follows:

$$\hat{G}(\boldsymbol{x},\boldsymbol{y},\omega)=\int_{-\infty}^{\infty}G(\boldsymbol{x},t;\boldsymbol{y},\tau)\mathrm{e}^{\mathrm{i}\omega(t-\tau)}\mathrm{d}t=\frac{1}{4\pi R}\mathrm{e}^{\mathrm{i}\mu E} \quad (14)$$

In the equation, $\boldsymbol{y}$ and $\boldsymbol{x}$ are the source point and the field point, respectively. $R=\sqrt{(y_1-x_1)^2+\beta^2(y_2-x_2)^2+\beta^2(y_3-x_3)^2}$, where $\beta^2=1-M^2$, $M=U/c_0$, is the Mach number in uniform flow; $E=R+M(y_1-x_1)$; $\mu=\kappa/\beta^2$, where $\kappa=\omega/c_0$, is the acoustic wavenumber; ω is the angular frequency; and i is the imaginary unit.

If the viscous stress e_{ij} is neglected and the contribution of the quadrupole sound source can be ignored at the subsonic speed, since the third term of the right side of Eq. (12) is the radiationless steady pressure [14], which has no effect on the sound radiation pressure, Eq. (12) can be simplified as follows:

$$p(\boldsymbol{x},t)=-\int_{-T}^{T}\iint_{S(\tau)}p_{\mathrm{s}}(\boldsymbol{y},t)n_i\frac{\partial}{\partial y_i}G(\boldsymbol{x},t,\boldsymbol{y},t)\mathrm{d}S(\boldsymbol{y})\mathrm{d}\tau \quad (15)$$

where $p_{\mathrm{s}}=(p-p_0)$, is the fluctuating pressure. We take the Fourier transforms on both sides of Eq. (15) with respect to the time t, and obtain the frequency domain equation of sound pressure for any point in the field as follows:

$$\hat{P}(\boldsymbol{x},\omega)=\iint_{S}\hat{P}_{\mathrm{s}}(\boldsymbol{y},\omega)[-n_i\frac{\partial}{\partial y_i}\hat{G}(\boldsymbol{x},\boldsymbol{y},\omega)]\mathrm{d}S(\boldsymbol{y}) \quad (16)$$

From the frequency domain Green function of Eq. (14), we have

$$\frac{\partial}{\partial y_j}\hat{G}(\boldsymbol{x},\boldsymbol{y},\omega)=[-\frac{y_1-x_1}{R^2}-\mathrm{i}\mu(\frac{y_1-x_1}{R}+M)]\hat{G}(\boldsymbol{x},\boldsymbol{y},\omega);\quad j=1$$

$$\frac{\partial}{\partial y_j}\hat{G}(\boldsymbol{x},\boldsymbol{y},\omega)=[\frac{\beta^2}{R}+\mathrm{i}\kappa](-\frac{y_j-x_j}{R})\cdot\hat{G}(\boldsymbol{x},\boldsymbol{y},\omega)\quad j=2,3 \quad (17)$$

We rewrite $\hat{P}_{\mathrm{s}}(\boldsymbol{y},\omega)$ in Eq. (16) as the wavenumber domain form. Then, we have

$$\hat{P}_{\mathrm{s}}(\boldsymbol{y},\omega)=\frac{1}{2\pi}\int_{-\infty}^{\infty}\int_{-\infty}^{\infty}\hat{P}_{s}(k_{\mathrm{s}},k_{\mathrm{t}},\omega)\mathrm{e}^{\mathrm{j}(k_{\mathrm{s}}\eta_{\mathrm{s}}+k_{\mathrm{t}}\eta_{\mathrm{t}})}\mathrm{d}k_{\mathrm{s}}\mathrm{d}k_{\mathrm{t}} \quad (18)$$

where j is the imaginary unit; η_{s} and η_{t} are the coordinates in the flowing direction and the spanwise direction of the airfoil surface, which correspond to y_1 and y_2 if the surface is a plane (see the coordinate system in Fig. 3).

According to Eqs. (16) and (18), we can obtain the pressure power spectrum of any point $\boldsymbol{x}$ in the field, $S_{\mathrm{pp}}(\boldsymbol{x},\omega)$, as follows:

$$S_{\mathrm{pp}}(\boldsymbol{x},\omega)=\int_{-\infty}^{\infty}\int_{-\infty}^{\infty}\left|H_{\mathrm{p}}(x,k_{\mathrm{s}},k_{\mathrm{t}},\omega)\right|^2S_{\mathrm{qq}}(k_{\mathrm{s}},k_{\mathrm{t}},\omega)\mathrm{d}k_{\mathrm{s}}\mathrm{d}k_{\mathrm{t}} \quad (19)$$

where $S_{\mathrm{qq}}(k_{\mathrm{s}},k_{\mathrm{t}},\omega)$ is the wavenumber-frequency spectrum of the fluctuating pressure at the source point $\boldsymbol{y}$ (wall surface). We define H_{P} as the radiation transfer function with the following expression:

$$H_{\mathrm{P}}(\boldsymbol{x},\boldsymbol{k},\omega)=\frac{1}{2\pi}\iint_{S}\left(-n_i\frac{\partial}{\partial y_i}\hat{G}(\boldsymbol{x},\boldsymbol{y},\omega)\right)\cdot\mathrm{e}^{\mathrm{j}(k_s\eta_s+k_t\eta_t)}\mathrm{d}S(\boldsymbol{y}) \quad (20)$$

Finally, we define the radiated sound pressure level at the field point $\boldsymbol{x}$ as follows [14]:

$$SPL=10\lg\frac{4\pi S_{\mathrm{pp}}(\boldsymbol{x},\omega)}{p_{\mathrm{ref}}^2} \quad (21)$$

where p_{ref} is the reference sound pressure, and $p_{\mathrm{ref}}=2\times10^{-5}$ Pa; the factor 4π is due to the one-sided spectrum transform and that the frequency unit is transformed from rad/s into Hz.

3 Numerical calculation model and results analysis

The research object of this paper is the NACA 0012 airfoil, which has been studied by Brooks et al. [9]. The chord length is 0.304 8, and the span is 0.475 2. It moves along the $-y_1$ direction with the velocity U, the Mach number M=0.208, and the angle of attack α=4°. The convective velocity coefficient c_u =0.8 is adopted. Fig. 3 shows the adopted suction surface (i.e., the upper surface) meshes of the NACA 0012 airfoil used in the numerical calculation. The coordinate origin is taken at the midpoint of the trailing edge. If the unit scale l_{e} is required to be less than 1/10 of the wavelength of the sound wave (here, we analyze the frequencies below 3 000 Hz), the unit scale $l_{\mathrm{e}}\leqslant c_0/(10f)$ = 11.5 mm.

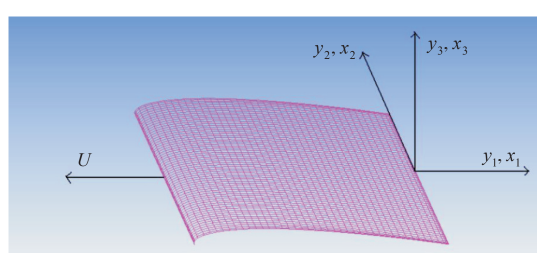

Fig.3 Mesh on the upper surface of the airfoil

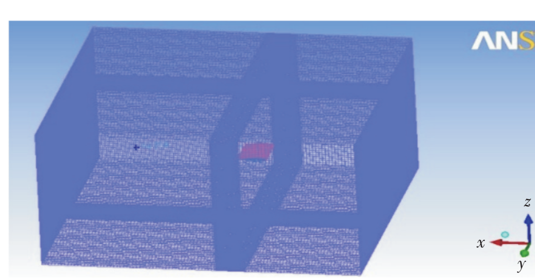

Fig.4 Computational domain model of airfoil motion

Here, we take the maximum mesh scale of 8 mm and divide the airfoil into 5 720 quadrilateral elements and 5 940 nodes. Fig. 4 shows the corresponding calculation domain model for the flow field, where there are 1 848 590 nodes and 1 890 768 hexahedral elements in total.

In order to verify the rationality of the mesh division, we first calculate the average pressure coefficient distribution on the upper and lower surfaces of the model (see Fig. 5): $C_{\mathrm{P}}=(p-p_0)/(0.5\rho U^2)$, where ρ is the gas density. The horizontal ordinate of Fig. 5 is the dimensionless value of chord length along the flowing direction $X=\boldsymbol{x}/c$, where c is the chord length. In order to compare with the test results [15], we set the angle of attack α as 5°. The pressure in the test is the measured value with $h/c=0.05$ (h is the height away from airfoil surface), which is considered to be approximately equal to the pressure value of the airfoil surface. From Fig. 5, we can see that the simulation results agree well with the test values.

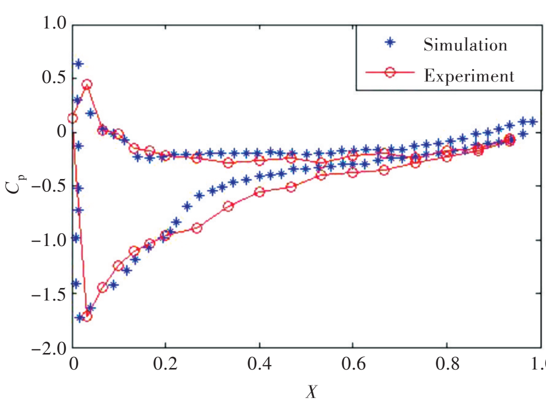

Fig.5 Pressure coefficient distributions of the upper and lower surface of the airfoil

By means of the flow field calculation and data processing, we obtain the wavenumber-frequency spectrum of the fluctuating pressure on the airfoil surface[16], and the result is shown in Fig. 6. Figs. 6(a) and 6(b) are wavenumber-frequency spectra of the pressure surface at 1 000 Hz, while Figs. 6(c)–6(f) are the wavenumber-frequency spectra of the pressure surface and suction surface at 1 200 Hz, respectively. From Figs. 6(b) and 6(d), we can see that, the maximum peak appears near the place where $k_{\mathrm{s}}U_{\mathrm{c}}/\omega_0$ is slightly larger than 1. This is because the effect of the shear stress on the wall surface leads to the migration of the wavenumber-frequency spectrum peak[17]. Comparing Figs. 6(d) with Fig. 6(f), we find that, due to the existence of the angle of attack, the wavenumber spectra of the pressure surface and the suction surface are not symmetric, and the energy of the pressure surface is higher than that of the

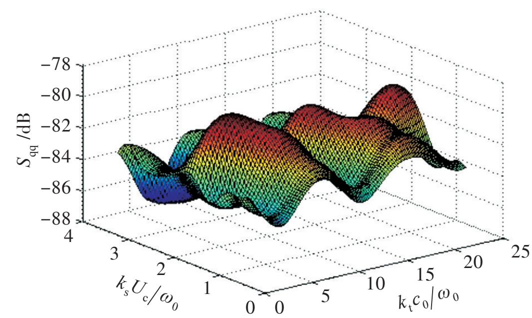

(a) Three-dimensional diagram of the wavenumber-frequency spectrum(f=1 000 Hz, pressure surface)

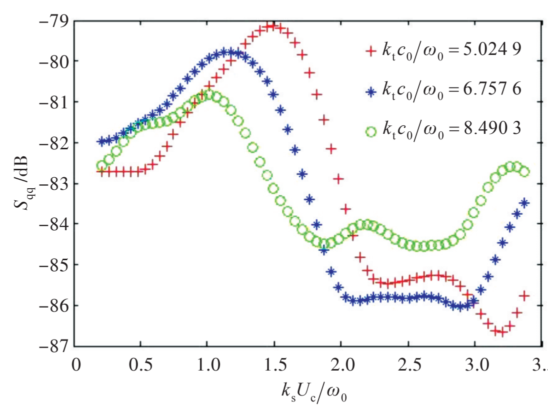

(b) Curves of the wavenumber-frequency spectra with the wavenumber change along the flowing direction (f=1 000 Hz, pressure surface)

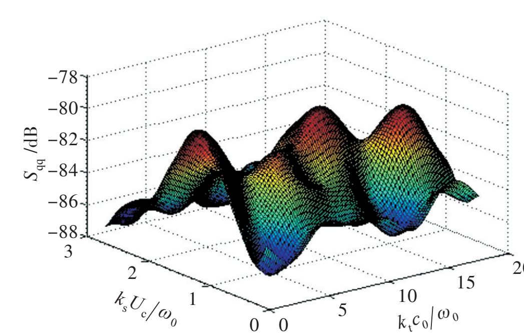

(c) Three-dimensional diagram of the wavenumber-frequency spectrum(f=1 200 Hz, pressure surface)

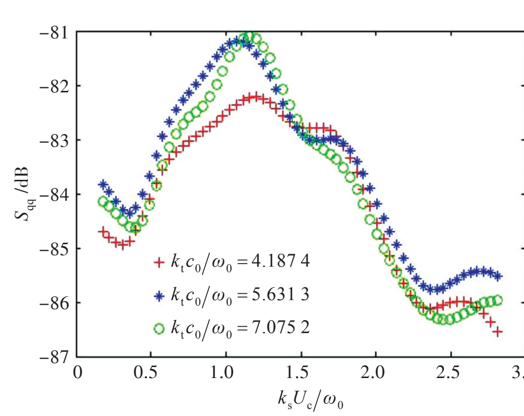

(d) Curves of the wavenumber-frequency spectra with the wavenumber change along the flowing direction (f=1 200 Hz, pressure surface)

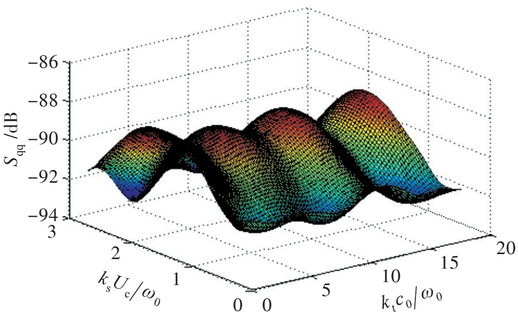

(e) Three-dimensional diagram of the wavenumber-frequency spectrum(f=1 200 Hz, suction surface)

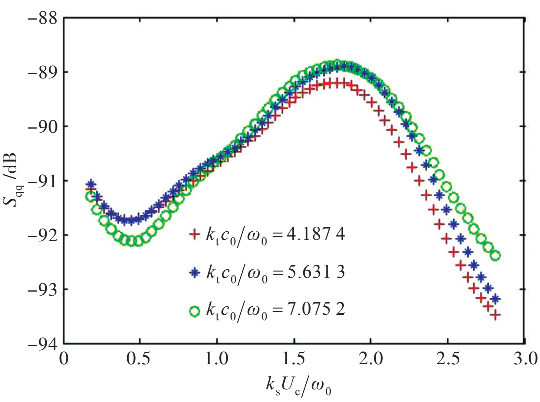

(f) Curves of the wavenumber-frequency spectra with the wavenumber change along the flowing direction (f=1 200 Hz, suction surface)

Fig.6 Numerical results of wavenumber-frequency spectrum on NACA 0012 airfoil

suction surface.

We substitute the above numerical calculation results of the wavenumber-frequency spectrum of the fluctuating pressure on the airfoil surface into the acoustic prediction equation in Section 2, and obtain the radiated sound pressure level of flow noise at the field point (0, 0, 1.22). Meanwhile, we use the acoustics software to calculate the radiated sound pressure level of flow noise at the same receiving point and under the same conditions. Then, the two results are compared with Brooks' empirical formula for the radiation noise of the NACA 0012 model (see Fig. 7). From the comparison of the results calculated by the software and obtained from Brooks' empirical prediction shown in the figure, we can see that, at the frequencies above 1 000 Hz, the differences among the sound pressure levels are basically within 8 dB; however, in the low frequency band, especially below 500 Hz, the results are quite different. The prediction results of this paper based on the wavenumber-frequency spectrum at the frequencies below 500 Hz agree well with the results from Brooks' empirical prediction, and the differences between the results obtained by this paper and those from Brooks' empirical prediction at the frequencies between

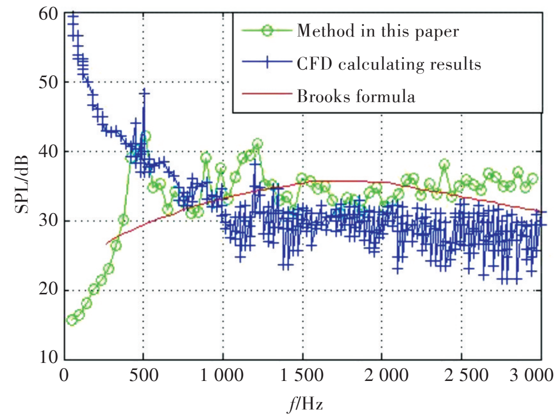

Fig.7 Comparison of flow noise with Brooks empirical prediction results

500 Hz and 3 000 Hz are basically within 6 dB. Therefore, compared with the results from Brooks' empirical prediction, in middle and low frequency bands, the flow noise based on the wavenumber-frequency spectrum prediction provided in this paper is closer to the fitted values than the results calculated by software.

4 Conclusion

In this paper, based on the wavenumber-frequency spectrum of turbulent fluctuating pressure, we provide a frequency domain method for flow noise prediction. Through the comparison of the results calculated by acoustics software and from Brooks' empirical formula, we find that the calculation results of the proposed method and the software are similar, e.g., there are equal peak frequencies (near 500 Hz and 1 200 Hz) within 500-1 500 Hz. There are also differences, e.g., the change tendency within 500 Hz is completely different from that of the results calculated by software, but is basically consistent with the change tendency of the results from Brooks' empirical formula. In conclusion, in this paper, we take the NACA 0012 airfoil as an example, take the wavenumber-frequency spectrum as the entry point, and obtain the numerical method for the wavenumber-frequency spectrum of the wall fluctuating pressure in the turbulent boundary layer. Theoretically speaking, it is applicable to any form. It not only extends the wavenumber-frequency spectrum model on a flat plate, but also has the generality. In addition, we take the calculation of aerodynamic noise as an example to predict the flow noise based on the wavenumber-frequency spectrum and the acoustic analog equation of the Goldstein version, which is independent of acoustic computing software. The results show that the forecast results of the method in this paper accord better with the experimental results at low and medium frequencies. Theoretically speaking, this is also applicable to hydrodynamic noise calculation. Therefore, we intend to extend this method to the flow noise calculation of different underwater vehicles in the next step.

References

[1] CORCOS G M. Resolution of pressure in turbulence [J]. Journal of the Acoustical Society of America, 1963, 35(2): 192-199.

[2] LI H, LIU C W, WU F L, et al. A review of the progress for computational methods for hydrodynamic noise[J]. Chinese Journal of Ship Research, 2016, 11(2): 72-89 (in Chinese).

[3] WANG C, ZHEN X L, ZHANG L X, et al. Prediction of submarine noise based on LES and infinite element method[J]. Noise and Vibration Control, 2015, 35(1): 1-6 (in Chinese).

[4] PAN Y C, ZHANG H X. LES method for investigation of noise generated by turbulent boundary layer [J]. Journal of Ship Mechanics, 2009, 13(6): 990-1001.

[5] ITO M. Improvement to the aerodynamic characteristics of shinkansen rolling stock[J]. Journal of Rail and Rapid Transit, 2000, 214(3): 135-143.

[6] MORITOH Y, ZENDA Y. Aerodynamic noise of high speed railway cars[J]. Japanese Railway Engineering, 1994, 34(1): 5-9.

[7] XIAO Y G, KANG Z C. Numerical prediction of aerodynamic noise radiated from high speed train head surface [J]. Journal of Central South University (Science and Technology), 2008, 39(6): 1267-1272 (in Chinese).

[8] WANG C X, ZENG G W, XU J. A comparative study of models for the wavenumber-frequency spectrum of TBL fluctuation pressure[J]. Chinese Journal of Ship Research, 2011, 6(1): 152-158 (in Chinese).

[9] BROOKS T F, HODGSON T H. Trailing edge noise prediction from measured surface pressures[J]. Journal of Sound and Vibration, 1981, 78(1): 69-117.

[10] CHASE D M. A model wavevector-frequency spectrum of turbulent-boundary-layer wall pressure[J]. Journal of the Acoustical Society of America, 1979, 65(Supp 1): S90.

[11] HOWE M S. Acoustics of fluid-structure interactions [M]. Cambridge: Cambridge University Press, 1998.

[12] ECKERT E R G, DRAKE R M. Heat and mass transfer [M]. 2nd ed. New York: McGraw-Hill Book Company, 1959.

[13] GOLDSTEIN M E. Aeroacoustics[M]. New York: Hill Book Company, 1976.

[14] ZHOU Q D. Broadband noise prediction of an airfoil or hydrofoil based on a frequency-domain formulation [J]. Journal of Hydrodynamics, 2003, 18 (3): 253-260 (in Chinese).

[15] WANG D F, DAI Q. Experimental research on the aerodynamics of a symmetrical airfoil near free surface [J]. Journal of Hydrodynamics, 2010, 25 (5): 703-710 (in Chinese).

[16] WU H L, ZHOU Q D, PAN Y C. Wave number-frequency spectrum of turbulent fluctuating pressure on airfoil surface[C]//Proceedings of the 24th International Congress on Sound and Vibration, 2017.

[17] LI F X, ZHANG Y W. Wavenumber frequency spectrum of the turbulent boundary layer wall pressure of a plate at acoustic and subconvective wavenumbers [J]. Journal of Northwestern Poly technical University, 1999, 17(2): 9-14 (in Chinese).

基于湍流脉动压力的波数—频率谱预报流噪声

伍宏亮[1]，周其斗[1]，吕晓军[1]，孟庆昌[2]

1 海军工程大学 舰船工程系，湖北 武汉 430033

2 海军工程大学 理学院，湖北 武汉 430033

摘　要：[**目的**] 根据Lighthill声类比方程及其发展理论，可以将壁面湍流脉动压力的波数—频率谱作为声源项来预报流噪声，且分析湍流脉动压力的波数—频率谱有助于了解湍流结构的时空关联特性。[**方法**] 以NACA 0012翼型为例，采用大涡模拟(LES)方法进行流场仿真计算，然后通过Fourier变换得到壁面湍流脉动压力波数—频率谱的数值解，并与Corcos的平板湍流边界层脉动压力波数—频率谱模型进行比较；在此基础上，将该波数—频率谱作为声源输入，代入Goldstein版本的声类比方程中预报辐射噪声，并与软件计算的流噪声结果以及Brooks试验拟合结果进行比较。[**结果**] 结果发现：小曲率变化的NACA 0012翼型表面的波数—频率谱具有与平板表面相似的一般特性；在中、低频段采用该方法预报的流噪声结果与Brooks试验结果拟合更好。[**结论**] 所得结果表明开展波数—频率谱研究是有必要的，将其作为主要声源项来预报亚声速下产生的流噪声是合理的。

关键词：波数—频率谱；Fourier变换；流噪声；声类比方程